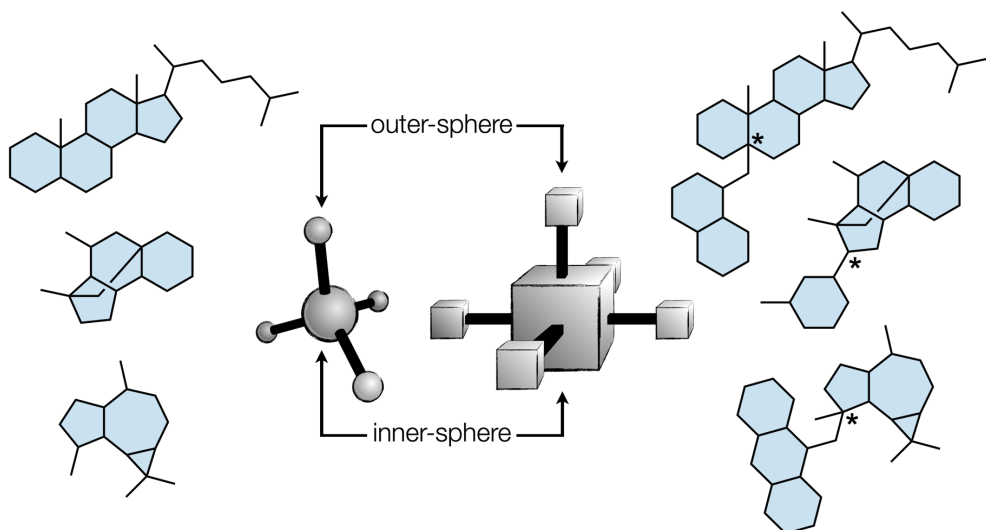


Inner- and outer-sphere cross-coupling of high F_{sp3} fragments

Simona Kotesova^{1,2} and Ryan A. Shenvi^{*,1}

¹Department of Chemistry, Scripps Research, La Jolla, California 92037, United States.

²Graduate School of Chemical and Biological Sciences, Scripps Research, La Jolla, California 92037, United States.



CONSPECTUS: Natural products research derives from a desire to explore, understand, and perturb biological function with atomic precision. To reach these goals at all, let alone efficiently, requires thoughtful, strategic, and creative problem solving. Often this means bold and unprecedented disconnections that would simplify access to complex structures, if only the methods existed to bridge these theoretical gaps. Whereas biological interrogations provide long-term intellectual value and impetus, methods come as attractive fringe benefits of natural product synthesis. This Account describes strategic, methodological solutions to

the syntheses of natural products—(−)-eugenial C, *Galbulimima* alkaloids GB18, GB22, GB13, and himgaline—featuring new, convergent disconnections as important problem-solving steps, which themselves were inspired by recent methods that arose from our group. Each target required the invention of first row transition metal-catalyzed cross-coupling procedures to satisfy the biological goals of the project. In these cases, synthetic strategy identified the methodological gap—the absence of stereo- and chemoselective couplings of appropriate fragments—but the tactical advantage conferred by first row metals met the challenge. These methods were competent to handle the dense, sterically encumbered motifs common to natural products, due to, in many cases, elementary steps that did not require bond formation between the hindered substrate and the metal center. Instead, these sterically lenient reactions appeared to involve metal–ligand–substrate reactions (i.e. outer-sphere steps), in contrast to the metal–substrate, coordinative reactions of precious metals (i.e. inner-sphere steps). Key observations from our previous studies, combined with the observations in seminal publications from other labs (Mattay, Weix, MacMillan), led to the optimization of ligand-controlled, stereoselective reactions and the introduction of complementary catalytic cycles that revealed new modes of reactivity and generated novel structural motifs. Optimized access to bioactive natural product space accelerated our timeline of biological characterization, fulfilling a common promise of natural products research. The integration of complex natural product synthesis, diversification and bioassay into a single PhD dissertation would have been unmanageable in a prior era. The unique ability of first row transition metals to effect Csp³-Csp³ cross-coupling with high chemo- and stereoselectivity has significantly lowered the barrier to reach the avowed goal of natural product synthesis

and reduced the burden (real or perceived) of integrating natural products into functional campaigns.

KEY REFERENCES:

- Kotesova, S.; Gan, X.-c.; Castanedo, A.; Green, S. A.; Shenvi, R. A. Iron-catalyzed hydrobenzylolation: stereoselective synthesis of (–)-eugenial *C. J. Am. Chem. Soc.* **2023**, *145*, 15714–15720.¹ *Two sequential outer-sphere reactions—MHAT and SH2—were proposed as the basis for stereoselective hindered fragment coupling.*
- Shevick, S. L.; Wilson, C. V.; Kotesova, S.; Kim, D.; Holland, P. L.; Shenvi, R. A. Catalytic hydrogen atom transfer to alkenes: a roadmap for metal hydrides and radicals. *Chem. Sci.* **2020**, *11*, 12401–12422.² *This collaborative review outlined mechanistic considerations for MHAT, including inner- vs. outer-sphere reactions and solvent cage effects.*
- Green, S. A.; Huffman, T. R.; McCourt, R. O.; van der Puyl, V.; Shenvi, R. A. Hydroalkylation of Olefins to form Quaternary Carbons. *J. Am. Chem. Soc.* **2019**, *141*, 7709–7714.³ *Mn/Ni dual-catalysis allowed alkenes to be quaternized by alkyl halides and established Mn(III) β -diketonates and phenylsilane as an effective reducing system for nickel.*

1. Introduction: Cross-coupling methods that employ first row transition metals offer orthogonal reactivity to second and third row metals. Whereas the latter, precious metals, often undergo coordinative reactions via canonical, two-electron elementary steps, the former, abundant metals, can generate and engage open shell carbon intermediates via outer-sphere steps.⁴ Here, the outer-sphere cross-couplings enable the formation of congested motifs in a chemoselective⁵ fashion and with great chemofidelity.⁶ Our group has developed a suite of hydrofunctionalizations enabled by one or two base metal catalysts that engage olefins and diverse coupling partners in unprecedented reactions (Figure 1a). These new methods have paved the way for convergent syntheses of natural

products that present interesting biological questions (Figure 1b). In turn, the demands of complex syntheses have inspired the development of novel cross-coupling methods (Figure 1c), driven by the need for chemo-, regio- and stereoselectivity. This account will detail how the interplay between new method development and natural product synthesis for biological interrogation contributed to innovation in the field of first-row metal-mediated cross-coupling.

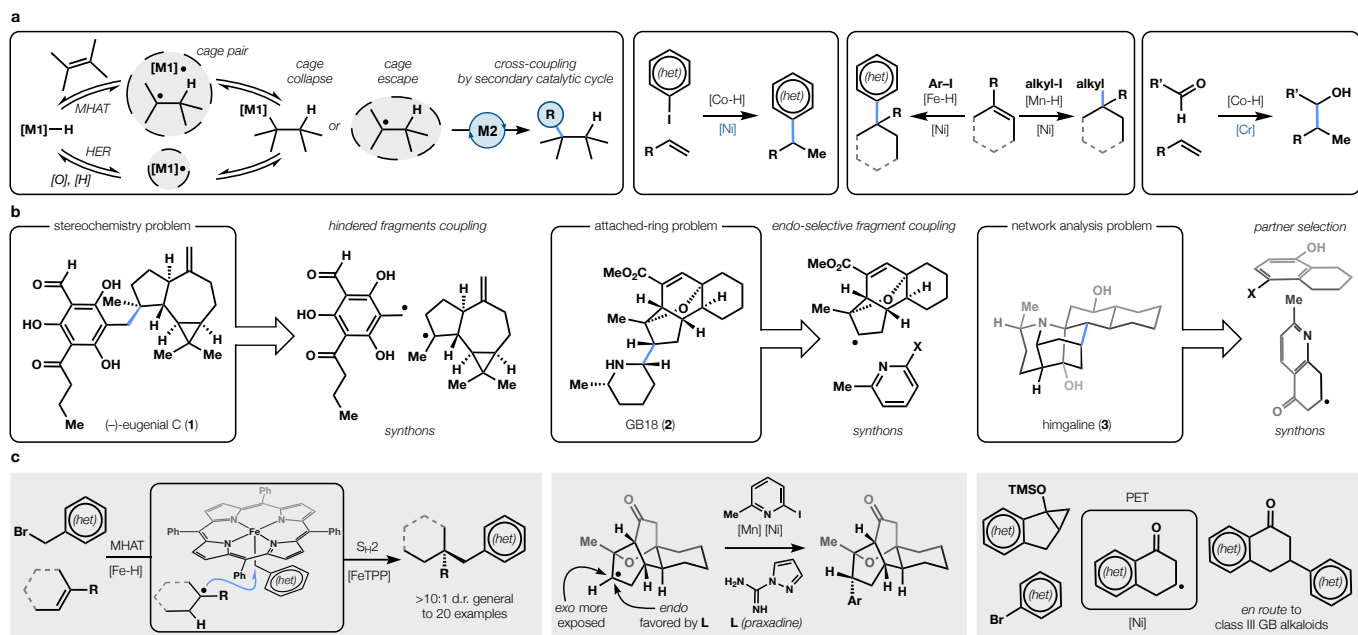


Figure 1. Overview of the Account. **a.** First-row transition metal-catalyzed cross-couplings enable general new methods involving MHAT as an outer-sphere elementary step; **b.** lessons learned from this work helped address problems in natural product chemical space: fragment coupling, stereoselectivity, strategic bond formation identified by network analysis; **c.** in turn, these disconnections led to general new methods.

2. Alkene hydrofunctionalizations by outer-sphere cross-coupling:

Formation of quaternary carbon stereocenters via Csp^3 - Csp^3 cross-coupling ranks among the most challenging of reactions.⁷ We thought carbon quaternization by alkene hydrofunctionalization might serve as a laudable goal due to its potential generality. After all, most

quaternary carbons contain adjacent C–H bonds.⁸ Furthermore, alkenes represent abundant feedstocks so their direct quaternization would circumvent substrate prefunctionalization steps. The difficulty of devising a general reaction also held appeal as we might learn new lessons in catalysis. Methods emanating from Drago-Mukaiyama hydration^{9,10,11,12,13,14,15,16,17,18} offered a powerful entry into this area due to their robustness,¹⁹ chemoselectivity⁵ and chemofidelity.⁶ These reactions have been hypothesized to proceed via metal-hydride hydrogen atom transfer (MHAT),²⁰ an outer-sphere elementary step that directly generates carbon-centered radicals (open shell carbon intermediates) from alkenes.²¹ MHAT tends to tolerate alkene poly-substitution, steric repulsion, and Lewis basic functional groups to a higher degree than inner-sphere, coordinative pathways characteristic of precious metals.^{6,22,20} Therefore, MHAT is a particularly powerful reaction pathway for complex, natural product-like substrates, which is where our interest originated.^{6,22,23,24} Many of these reactions are catalyzed by commercially available first-row transition metals complexed with inexpensive ligands (acetylacetone, acac; dipivaloylmethane, dpm; etc.), providing a barrierless entry for any practitioner. In contrast to traditional metal hydrides with strong field supporting ligands (e.g. cyclopentadienyl, carbonyl, phosphine, and pyridine), that adopt low-spin electronic configurations, these metal hydrides with weak field ligands (acac, salen) adopt intermediate or high spin electronic configurations with unpaired electrons in antibonding orbitals.² Access to higher oxidation states facilitates homolysis to radical intermediates; supporting ligands can be labile; multiple spin states may be present; and bonds are often weaker. These properties have not been directly measured, in part because these weak field metal-hydrides are not isolable, but computational studies have begun to shed light on these mechanistic features. For example, a computational study by Hui Chen and co-workers suggests that iron(III)hydrides react with single-state reactivity as opposed to multi-state reactivity

involving spin cross-over.²⁵ Understanding these factors and their mechanistic consequences will be important for future reaction discovery.

Historically, MHAT-based methods have employed classical, stoichiometric radical traps to install heteroatomic functional groups.^{8,26} In contrast, variants from our group add a secondary transition metal complex to generate catalytic concentrations of a coupling partner that engages an open-shell carbon intermediate (Figure 1a). Despite its low concentration, the high rate-constant associated with capture of the carbon radical by the secondary metal species leads to efficient overall reaction.^{27,28} Nevertheless, different first-row transition metal catalysts enable complementary reactivity pathways and unique substrate tolerances based on competing elementary steps occurring at different rates. For example, MHAT dual catalysis was restricted initially to the formation of *sec*-alkyl arenes from terminal alkenes by cobalt salen-catalyzed hydroarylation, which appeared to proceed via *sec*-alkylcobalt transmetalation by an arylnickel.²⁹ The suitability and branched-selectivity of electron-neutral, -rich or -deficient alkenes (e.g., α -olefins, vinyl thioether, vinyl pinacol boronate) reflected the outer-sphere nature of the MHAT step, and the chemoselectivity of both cobalt and nickel catalysis allowed the use of substituted benzene electrophiles as well as heteroaromatics (Figure 2). The inherent instability of *tert*-alkyl cobalt salen complexes prevented formation of quaternary centers under similar conditions; instead, alkene isomerization occurred via reversible MHAT.

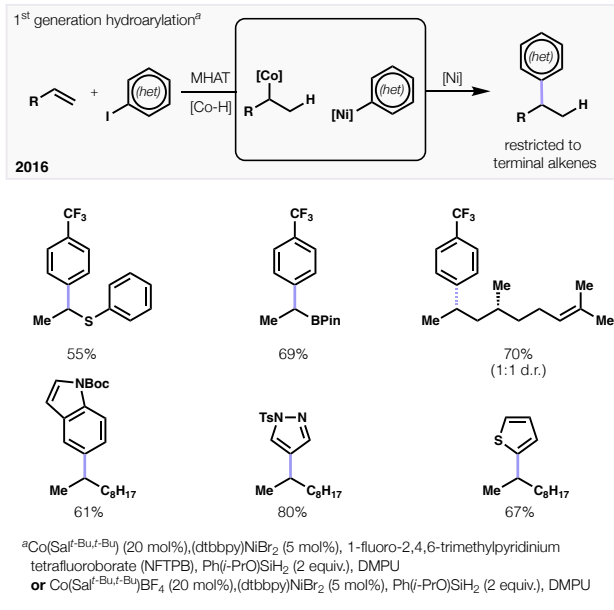
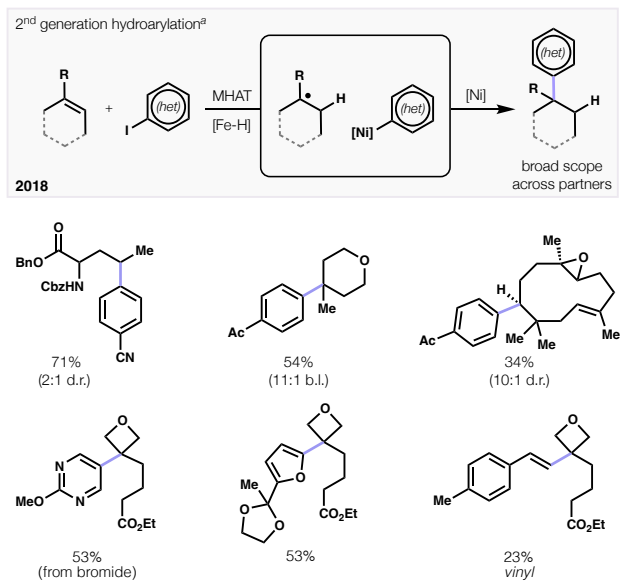


Figure 2. Initial forays into hydroarylation were restricted to terminal alkenes, reflecting the mechanism: radical collapse to a *sec*-alkyl organocobalt followed by transmetalation.

Replacement of cobalt salen with an iron β -diketonate complex expanded the hydroarylation methodology to include di-, tri- and even tetrasubstituted alkenes and form quaternary centers with broad scope.³⁰ We suspect that this breadth reflects the very low stability of the intermediate Fe–H complex, which appears to undergo rapid and irreversible MHAT.^{31,32,33,34,35,36} Holland has even suggested that metal hydride formation, not MHAT, is turnover limiting.^{41,37} Mechanistic differences in metal hydride formation arising from alternative ligand spheres may also contribute to varying substrate tolerance. For instance, metal acac complexes have been proposed to form metal hydrides through a concerted interchange mechanism,³⁷ which may not be possible for salen complexes lacking open *cis*-coordination sites.^{16,38,39,45} As a consequence of this rapid rate of alkene engagement, *sec*-alkyl and *tert*-alkyl arenes can be formed with ease from simple, electron-neutral olefins and haloarenes. In contrast to Brønsted or Lewis acid-mediated reactions like

Friedel-Crafts alkylation, a variety of acid-sensitive groups like furans, ketals, oxetanes and epoxides can be incorporated into substrates (Figure 3).

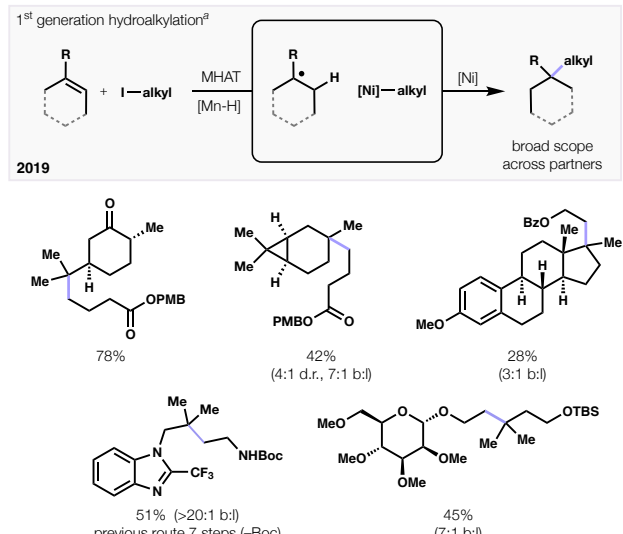


^aFe(dpm)₃ (30 mol%), NiBr₂(diglyme) (10 mol%), Mn⁰ (1 equiv.), MnO₂ (1 equiv.), Ph(i-PrO)SiH₂ (2 equiv.), DCE/NMP, 22 °C

Figure 3. Rapid and irreversible MHAT from iron hydrides allow quaternary center formation.

Combination of nickel and manganese β -diketonate catalysts enabled Csp³-Csp³ cross-coupling,³ likely due to the same irreversibility of Mn-catalyzed MHAT as with Fe. This reaction fulfilled a longstanding goal in the lab to realize a "carbo-Menshutkin" reaction, i.e., quaternization of a simple alkene with an alkyl halide by analogy to the quaternization of an amine (Figure 4). In this case, efficient conversion relied on the combined use of manganese and nickel. Consistent with prior work,^{4,40} we suspect nickel promotes conversion of the alkyl iodide to the corresponding radical *en route* to alkynickel formation and capture by the tertiary radical produced by MHAT. Thus, Co-, Fe- and Mn-catalyzed MHAT could be leveraged in Csp²-Csp³ and Csp³-Csp³ cross-coupling reactions that benefited from the remarkable mildness of first-row transition metal catalysis. This Mn/Ni dual-catalyzed hydroalkylation enabled the first use of an sp³-hybridized electrophile (alkyl halide) among MHAT hydrofunctionalizations. Here, the hindered Mn(dpm)₃

ensured an optimal rate of MHAT to intersect the nickel/manganese catalytic cycles that engage the alkyl halide. HFIP and potassium carbonate proved to be crucial additives hypothesized to facilitate σ -bond metathesis from phenylsilane to the Mn β -diketonate, possibly via formation of a transient alkoxy silane.⁴¹ The reaction displayed exceptional functional group compatibility in its tolerance of esters, phthalimides, carbamates, silyl enol ethers, boronic esters, and epoxides (Figure 4). A broad range of terpenoids were successfully functionalized, enabling the transformation of simple or complex, electron-neutral alkenes. A diverse range of alkyl halides could be appended that included sensitive functional groups such as acetals, nitrogen-containing heterocycles and numerous chain lengths. The use of nickel, however, suggested some deficits: its high toxicity proscribed large scale application⁴² and steric crowding of ligands about the metal suggested that more encumbered partners might resist coupling. As seen in Section 3, this second limitation was confirmed and required intersection with an alternative catalytic cycle to couple hindered partners.



^aMn(dpm)₃ (20 mol%), Ni(acac)₂ (2.5 mol%), HFIP (2 equiv.), K₂CO₃ (3 equiv.), PhSiH₃ (3 equiv.), DCE/PC, 22 °C

Figure 4. Hydroalkylation required a manganese hydride catalyst, which reacted with the alkene by MHAT but also served to reduce the nickel catalyst.

Finally, the combination of MHAT catalysis with chromium enabled chemistry reminiscent of carbanion reactivity to form Csp^3 - Csp^3 bonds.⁴³ This bimetallic reaction signaled a departure from prior work in MHAT that led alkenes to undergo traditional radical or cationic polar crossover reactivity.^{44,45,46,47} Instead, the open-shell carbon intermediates were captured by chromium to form strong polar nucleophiles that could react with aldehydes with branched selectivity. Typically, chromium(II) serves as the active species to convert alkyl halides to alkylchromium(III) reagents for carbonyl addition,⁴⁸ which suggested that the chromium(III) salts were reduced *in situ*, either by the silane or intermediate cobalt hydride. Mechanistic experiments were consistent with an alkyl–cobalt(III) transmetalation to an alkyl–chromium(III), mediated by *in situ* generated chromium(II). In prior work,²⁷ the oxidant was implicated in rescue of the cobalt(III) catalyst, whose hydride (Co^{3+} –H) can undergo a hydrogen evolution reaction (HER) to the inactive Co(II) and must be brought back on-cycle via oxidation. The reaction scope included aromatic, heteroaromatic and aliphatic aldehydes with broad electronic variation, and tolerated reactive functional groups like esters, tosylates, and chlorides (Figure 5).

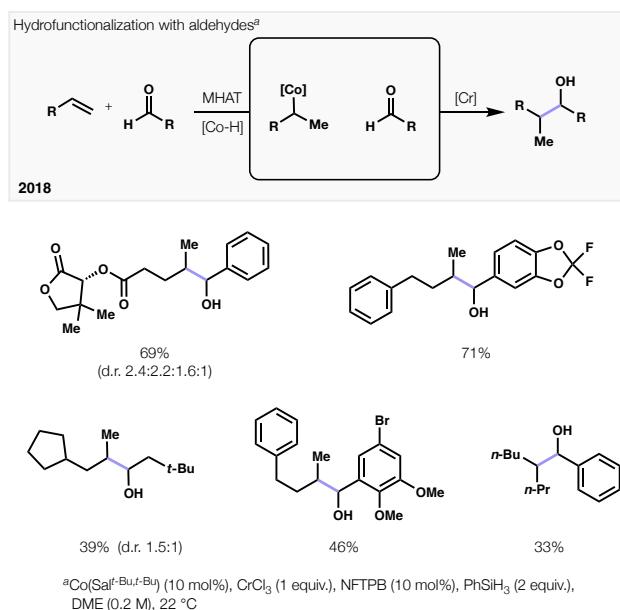


Figure 5. The mechanism of 1st generation hydroarylation inspired the use of chromium salts to transform unreactive organocobalt complexes to nucleophilic organochromium reagents.

Our foregoing research demonstrated that alkenes could undergo branch selective cross-coupling catalyzed by first-row transition metals. We hypothesized that intermediate metal hydrides might react with the alkenes via MHAT—still a controversial proposal due to the low BDE of metal hydrides necessary⁴⁹ and the competing HER that might be expected to predominate.⁵⁰ Among the several compelling arguments that the MHAT step occurs (an outer-sphere reaction), as opposed to alkene coordination/metal insertion (an inner-sphere reaction) is the observation that increased alkene substitution does not significantly decrease reaction rate.²² This steric tolerance lends itself to natural product synthesis, especially hindered, bi-lobed motifs common to meroterpenoids.⁵¹ A general solution, however, requires not merely effective alkene engagement, but also efficient capture of the ensuing radical, in addition to stereocontrol in the case of many quaternary carbon stereocenters prevalent in natural products. We were curious to explore whether dual catalytic MHAT cross-coupling could solve compelling problems in complex synthesis and how the methods might be improved when subjected to a challenging substrate pair. We did not expect this exercise to lead to the development of a new cross-coupling platform competent for the diastereoselective formation of hindered Csp³-Csp³ bonds.

3. Eugenial C via MHAT / S_H2: two outer-sphere steps for alkene hydrofunctionalization

Our proposal for the synthesis of meroterpenoid (–)-eugenial C (**1**) was married to the development of two generations of hydroalkylation methods,^{1,3} as well as the potential for these methods to interrogate the biological function of its two lobes.⁵² Biosynthetic reactions forge the unique bi-lobal structure of (–)-eugenial C convergently through Friedel-Crafts capture of a

phloroglucinolmethyl cation reaction by bicyclogermacrene, followed by carbocationic rearrangement (Figure 6, top left).⁵³ The generality and versatility of a biomimetic route seemed low. In contrast, an MHAT cross-coupling might provide a simple and combinatorial route to **1** and its many meroterpenoid congeners (Figure 6, top right). Retrosynthetic dissection of the stereogenic quaternary center would allow us to probe the biological function of each lobe, both in the context of the antimicrobial activity of **1** and as a general lysine adductor. An effective cross-coupling would enable these future biological goals. Perhaps the greatest challenge to surmount was skepticism from one of us (R.A.S.) that such a cross-coupling would ever be possible.

Initial forays into the synthesis of **1** were not encouraging and encountered material supply problems, low cross-coupling yields, no stereoselectivity and no catalyst turnover. As luck would have it, our chiral pool starting material, aromadendrene, suffered from COVID-19 pandemic-era shortages that left it backordered for months. Literature sleuthing identified a local tree, *Eucalyptus globulus*, that produced large quantities of aromadendrene and its hydrated counterpart,⁵⁴ globulol, in its woody fruits.^{55,56} The San Diego Natural History Museum's online Plant Atlas⁵⁷ identified major groves of *E. globulus* trees just a few miles from our laboratory, allowing us to devise an effective procedure for the collection, extraction, and isolation of materials for the alkene coupling partner. Synthesis of the hexasubstituted benzyl bromide partner proved challenging due to its *o,o'*-disubstitution, which significantly reduced yields of product relative to unsubstituted partners. Late stage *o,o'*-dihydroxylations were unsuccessful. Instead, we crafted a *bis*-dioxinone substrate that tied the *ortho*- substituents into a butterfly structure to decrease steric repulsion and reduce Lewis basicity (Figure 6, middle).

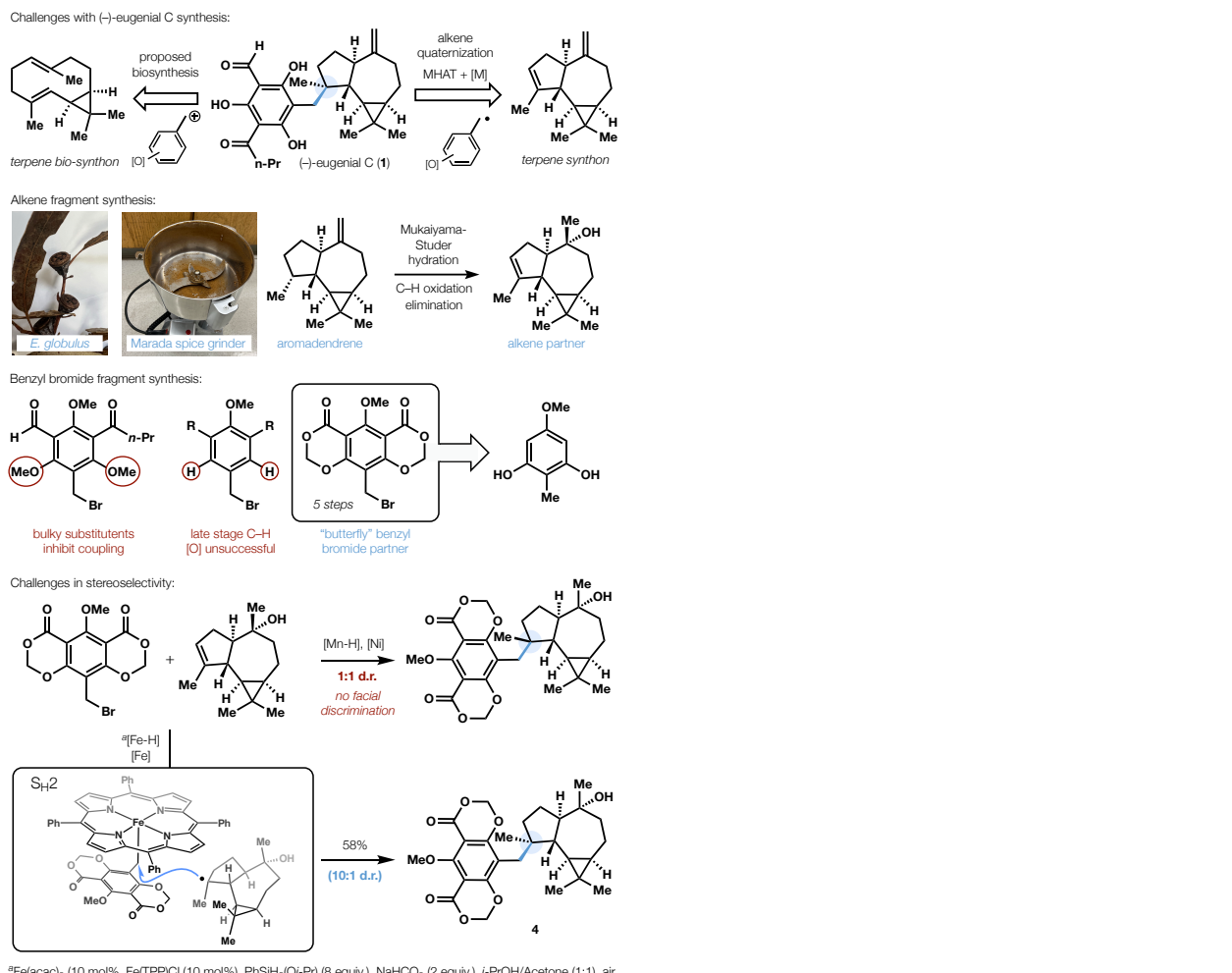
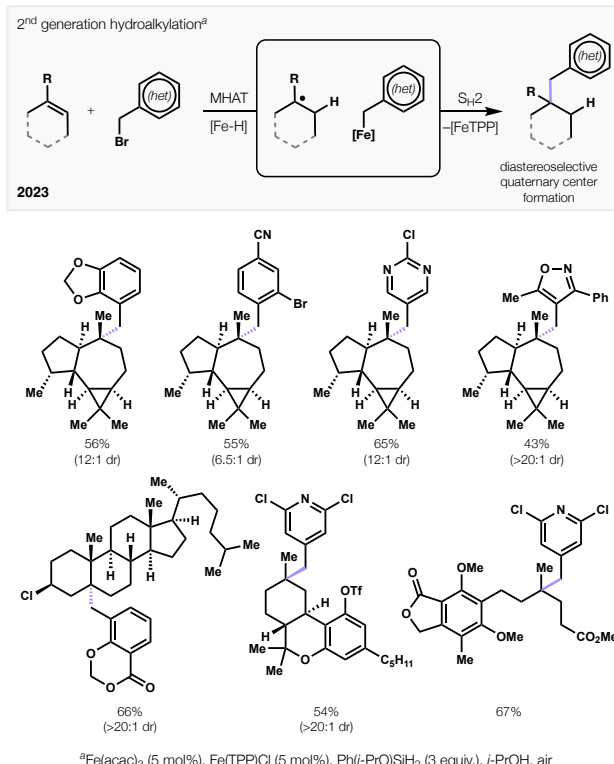


Figure 6. The strategy to synthesize antimicrobial meroterpenoid (-)-eugenial C evolved into a general method for MHAT/S_{H2} coupling.

Whereas this design led to some improvements in coupling efficiencies (20–30% yield), the metal loadings stayed high (0.5–1.0 equiv.) and stereoselectivity remained stuck at 1:1 d.r. across dozens of variations including diverse ligand sets and substrate-embedded directing groups. We considered that the mechanism of C–C bond formation might be destined to fail for three different reasons: reversibly-formed diorganonickel diastereomers underwent reductive elimination at equal rates, diorganonickel diastereomers formed irreversibly at equal rates, or benzyl halides represented a special case where direct radical-radical coupling led to mixtures of diastereomers. Thus, we sought an alternative bond-forming event via an S_{H2} step featured in a recent

photocatalytic Csp^3 - Csp^3 cross-coupling from the MacMillan lab.⁵⁸ Simple models suggested an intermediate benzyl porphyrin might encounter the distant steric environment at the radical's periphery and differentiate its prochiral faces. If successful, this approach would merge two outer-sphere elementary steps, MHAT and S_{H2} , to cross-couple simple building blocks and form a very hindered bond.

Despite the potential for multiple off-pathway processes—benzyl dimerization, alkene hydrogenation, radical oxidation—to contravene the productive reaction, coupling occurred effectively to deliver **4** with high diastereoselectivity (Figure 6, bottom). Iron proved more effective than manganese to promote good yields at low catalyst loading (5–10 mol%), likely due to the tendency for iron to turnover efficiently at low concentrations of O_2 ,³⁷ the lower hydridic character of Fe–H compared to Mn–H,^{2,20,33} and possibly the lower rate of hydrogen evolution reaction (HER)^{59,60} associated with Fe–H. A clear improvement in reactivity was also observed when exchanging bulky dpm ligands for acac, likely owing to a faster rate of the outer sphere MHAT step.^{38,61} Iron became the workhorse of a new reaction system that engaged alkenes in MHAT to form a tertiary radical, and formed a benzyl iron complex that underwent S_{H2} . The unusual breadth of the substrate scope is captured in Figure 7.



^aFe(acac)₃ (5 mol%), Fe(TPP)Cl (5 mol%), Ph(i-PrO)SiH₂ (3 equiv), *i*-PrOH, air

Figure 7. Iron-iron dual catalysis engages a breadth of 1,1-disubstituted and trisubstituted alkenes in two putative outer-sphere reactions: MHAT and S_{H2}.

The simplicity of the reaction suggests many new variants await discovery; the lower toxicity of iron compared to nickel commends this MHAT/S_{H2} coupling for large scale use.⁶² Developed in the context of (–)-eugenial C, most coupling partners were bound to be simpler and thus the iron-catalyzed hydrobenzylolation demonstrated broad applicability to a range of heavily functionalized, natural product derived alkenes and diverse bromomethyl (hetero)arenes. The stereoselectivity of the reaction proved general and, in most cases, featured diastereomeric ratios between 10:1 to 20:1 for any given substrate (Figure 7).

The optimized cross-coupling procedure afforded quick and scalable access to (–)-eugenial C in 4 additional steps; ongoing work has produced analogs to probe function like phenotypic effects and lysine adduction. By allowing the biological questions to dictate the needs of the synthesis, and the synthesis to drive innovation in cross-coupling, we arrived at a new direction for

methodological exploration and developed an efficient platform for biological interrogation. Biological assays are currently underway to verify the antibacterial activity of eugenial C, investigate the activity of its congeners and analogs, and probe the basis for these effects.

4. GB18: ligand control over attached-ring *endo*-selectivity

Observations and mechanistic hypotheses derived from the Mn/Ni dual-catalytic hydroalkylation manifested themselves in a crucial step of another natural product synthesis, this time in the context of a cross-electrophile coupling (XEC).⁶³ GB18 contains a difficult tetrahedral attached-ring problem: its pendant 6-methyl-piperidine resides on the *endo*-face of a tetracyclic scaffold; both attached-ring bridgeheads are stereogenic centers (Figure 8, top). This structure caught our attention due to its potent activity in a mouse grooming assay and a literature hypothesis that it might represent the hallucinogenic principle of *Galbulimima* (GB) bark.^{64,65,66,67} A cross-coupling solution to GB18 would accelerate access to large quantities of material for biological interrogation and offer an avenue for diversification to analogs to perturb pharmacology. This coupling, however, proved unusually challenging, again for reasons of chemo- and stereoselectivity. Intermediate **5** could be procured in 6 steps on multigram scale, but cross-electrophile coupling with 6-halo-picoline under a variety of standard conditions (Zn⁰, Mn⁰, TDAE) led to protodeiodination or ether fragmentation (Figure 8, middle). It's important to note that traditional precious metal-catalyzed arylations of **6** were unsuccessful. The iodide substituent of **5**, however, served as a homolytically-cleavable substituent on carbon that could undergo outer-sphere (relative to carbon) reactions with a reductant, analogous to the proposed, outer-sphere S_{H2} reactions^{68,69} available to organoporphyrins and carbon-centered radicals.⁷⁰

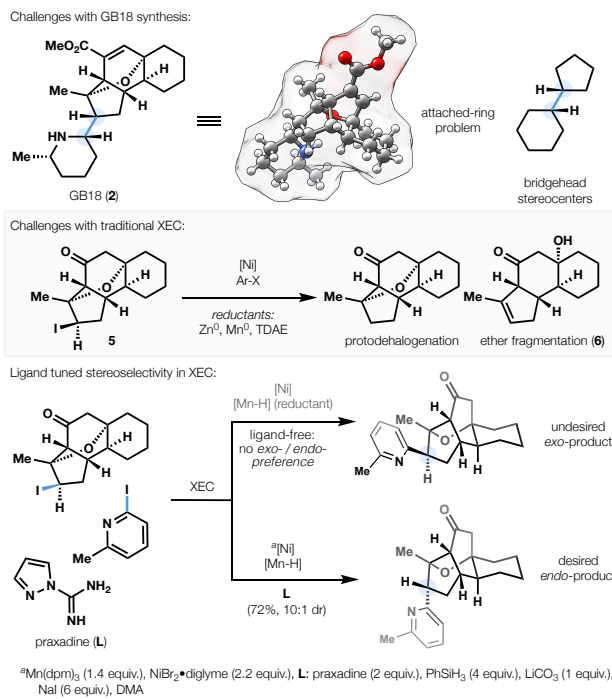


Figure 8. An attached-ring problem evolved into a need for stereo-invertive cross-coupling to append a picoline on a more hindered *endo*-face. This could be achieved with stereocontrol by an amidine ligand, which happened to be the inexpensive drug, praxadine.

Owing to the pioneering work of Weix, Reisman, and others, cross-electrophile coupling has been featured in a variety of complex syntheses, yet its application to the formation of an attached ring motif has little precedent and none for *endo*-selective coupling.^{71,72} Drawing inspiration from the lab's Mn/Ni dual-catalyzed hydrofunctionalization,^{Error! Bookmark not defined.} in which the MHAT catalyst $Mn(dpm)_3$ appears necessary to reduce nickel(II) to (I), we applied the same catalytic system to the cross-electrophile coupling of 5. Although coupled products were observed, diastereoselectivity was absent. Notably, the *endo*-isomer is destabilized by 0.5 kcal/mol relative to *exo*-, and model radical addition reactions occurred preferentially from the *exo*-face. Fortunately, a careful survey of amidine ligands, directly inspired by Weix's discovery of their privileged performance in cross-electrophile coupling,⁷³ unearthed a novel amidine ligand

(praxadine) that favored the more hindered *endo*-isomer by 10:1 over *exo*- (Figure 8, bottom). This ligand-controlled stereochemical inversion of iodide **5** represents an important step forward in generalized stereocontrol for organonickel/carbon radical capture independent of substrate topology. Even though this cross-electrophile coupling used the reagents of our hydroarylation, the underlying mechanism did not involve *in situ* formation of an alkene: subjection of this control substrate to the same reaction conditions yielded no product. The mechanism of stereocontrol could not be fully elucidated, however, and the complexity of the possible pathways prevented the development of catalytic conditions. We considered that the final diastereoselectivity may derive from a hydrogen-bond network between the pyridynickel-ligand complex and the Lewis basic oxygen bridge of **5**; however, this and related models remain speculative. Elaboration of the *endo*-product to GB18 identified μ - and κ -opioid receptors as high affinity targets, whereby GB18 served as a potent antagonist ($\text{pIC}_{50} = 8$) at both targets. The ease of cross-coupling **5** with stereocontrol lends this substrate to extensive diversification by heterocycles and investigation of opioid pharmacology with this novel class. Indeed, this approach has led to >90 analogs of GB18 currently under investigation *in vitro* and *in vivo*.

5. GB22, GB13 and himgaline: siloxycyclopropane *endo*-arylation

In contrast to the stereoselective attached-ring cross-coupling featured in the synthesis of GB18, a class I alkaloid, the alternative Class III GB alkaloids presented an altogether different attached-ring problem.⁷⁴ We had aimed to use the newly isolated aromatic alkaloid GB22 as a linchpin intermediate *en route* to more complex congeners like himgaline, and traced their syntheses back through hydrogenation and Friedel-Crafts transforms to compound **9** (Figure 9, top). Similar scaffolds had been synthesized in a single step via strong acid-mediated double Friedel-Crafts reactions (Figure 9, middle).⁷⁵ These reactions failed, however, due to incompatible arene

electronics and the acid sensitivity of the product. In order to circumvent the unproductive carbocation intermediate, we targeted the corresponding carbon radical with the anticipation that nickel could mediate its capture and cross-coupling with a bromoarene partner.

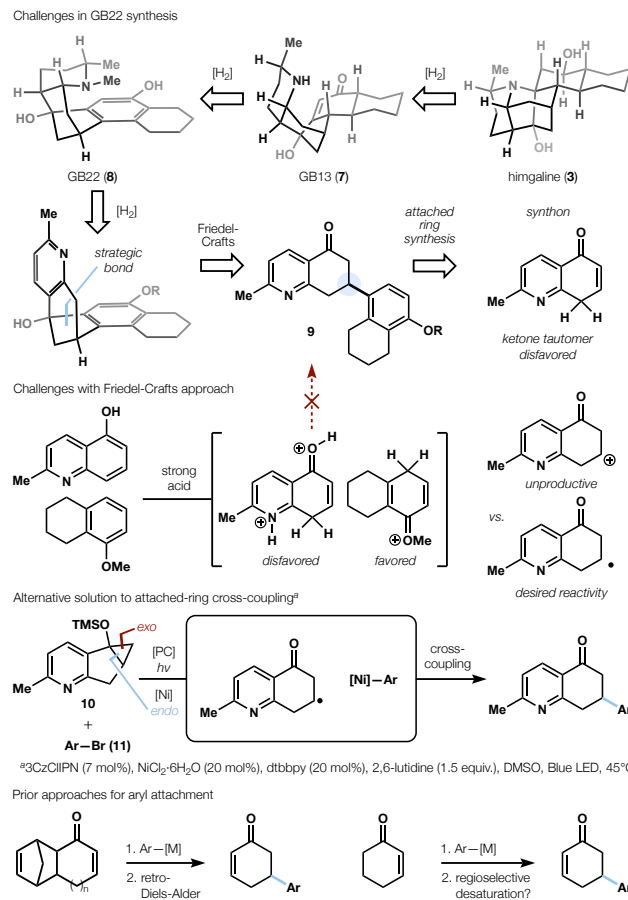


Figure 9. Himgaline could be retrosynthetically transformed to a bridging tetracycle, whose two strategic bonds could be dissected sequentially. The polar disconnection could be replaced with a new radical cross-coupling that complemented existing enone–arene attachment methods.

This convergent strategy would enable rapid access to the GB chemical space for biological exploration: in particular, the assignment of high affinity human receptors. We were inspired by Mattay's seminal work demonstrating that photoinduced electron transfer (PET) between arene dyes and siloxycyclopropanes results in the formation of β -keto radicals.⁷⁶ Capture by an

organonickel intermediate would result in net reversal of the normal regioselectivity of cyclopropanol arylations: palladium catalysts, for example, cleave the *exo*-bond on similar ring systems,⁷⁷ whereas this proposed nickel catalysis would select for the *endo*-bond (Figure 9, middle) as proposed by Lectka.^{78,79} Indeed, subjection of pyridine siloxycyclopropane **10** and arene **11** to Zhang's carbazole-cyano-benzene PET catalyst⁸⁰ (photocatalyst, PC) in the presence of a nickel catalyst led to serviceable yields of the targeted attached-ring system. This reaction proved general across variations to both partners and provided an alternative solution for the synthesis of 5-functionalized-2,3-unsaturated cyclohexenones. Typically, this general substructure can be synthesized by protection, unsaturation, conjugate addition and deprotection, by conjugate addition, followed by selective unsaturation, or by Robinson annulation. *Endo*-selective cyclopropane ring opening offered an effective solution in the case of **9**, where none of these alternatives were productive. The nickel-catalyzed attached-ring formation served as an effective tool for route discovery, enabling the efficient advance of **9** to GB 22, GB 13, and himgaline upon strategic scouting of an optimal final sequence.

CONCLUSION

The advantages of first-row transition metals lend themselves to the most challenging problems in natural product synthesis, especially the ability to cross-couple complex, high fraction sp³ (F_{sp³}) fragments with stereoselectivity, chemoselectivity and chemofidelity. This latter category, which describes the capacity of a reaction to occur independent of the molecular context of the reacting functional group, contrasts markedly with precious metal-catalyzed reactions of alkenes. Here inner-sphere, coordinative reactions exhibit extreme sensitivity to substitution patterns and steric repulsion from adjacent atoms, an effect minimized in MHAT reactions due to the outer-sphere nature of the reaction pathway. The new ability to combine MHAT with cross-coupling reactions

has enabled some startling results, starkly illustrated in the synthesis of (–)-eugenial C by its iron-catalyzed convergent cross-coupling of complex and hindered partners (Figures 6 and 7). Both the stereoselectivity and the efficiency of the cross-coupling likely benefit from two sequential outer-sphere reactions, MHAT and S_{H2} , and establish a thought-provoking paradigm for alkene functionalization. Additionally, the merger of MHAT with nickel catalysis offers solutions to related problems in fragment coupling, including tetrahedral attached-ring synthesis. These cross-coupling platforms to access (–)-eugenial C, GB18, GB22, GB13 and himgaline relate directly to goals in chemistry and biology, which continue to bear fruit as methods expand beyond the initial targets and the naturally-occurring scaffolds are diversified beyond nature's constraints.⁸¹ The view that total syntheses are vain tales of mountain climbing—full of sound and fury, symbolizing nothing—ring hollow if sights are set beyond mere target acquisition. Instead, new cross-coupling reactions can identify profitable areas of reactivity to mine on the mountain slopes and can illuminate paths to accelerate exploration beyond the summit.

AUTHOR INFORMATION

Corresponding Author

[*rshenvi@scripps.edu](mailto:rshenvi@scripps.edu)

Author Contributions

The manuscript was written through contributions of all authors.

Funding

This work was supported by grants from the NSF (CHE 1955922, CHE 2155228, CHE 1856747) and the NIH (GM122606, AT012075), as well as a generous Kellogg Fellowship to S.K.

Notes

The authors declare no competing financial interest.

Biographies

Simona Kotesova was born in Bratislava, Slovakia and grew up in the San Francisco Bay Area. She obtained her undergraduate degree from UC Berkeley and an MSc. in medicinal chemistry from the University of Copenhagen. She is currently a graduate student in the Shenvi lab at Scripps Research working at the interface of MHAT methodology development and natural product synthesis.

Ryan A. Shenvi was born and raised in Wilmington, Delaware. He earned his PhD with Phil Baran and undertook postdoctoral studies with E. J. Corey. He has been a faculty member at Scripps Research since 2010.

ACKNOWLEDGMENTS

We gratefully acknowledge the contributions of students, postdocs, and faculty, past and present, that have led to the research discussed herein.

REFERENCES

- ¹ Kotesova, S.; Gan, X.-c.; Castanedo, A.; Green, S. A.; Shenvi, R. A. Iron-catalyzed hydrobenzylolation: stereoselective synthesis of (–)-eugenial. *C. J. Am. Chem. Soc.* **2023**, *145*, 15714–15720.
- ² Shevick, S. L.; Wilson, C. V.; Kotesova, S.; Kim, D.; Holland, P. L.; Shenvi, R. A. Catalytic hydrogen atom transfer to alkenes: a roadmap for metal hydrides and radicals. *Chem. Sci.* **2020**, *11*, 12401–12422.
- ³ Green, S. A.; Huffman, T. R.; McCourt, R. O.; van der Puyl, V.; Shenvi, R. A. Hydroalkylation of Olefins to form Quaternary Carbons. *J. Am. Chem. Soc.* **2019**, *141*, 7709–7714.
- ⁴ Choi, J.; Fu, G. C. Transition Metal–Catalyzed Alkyl–Alkyl Bond Formation: Another Dimension in Cross-Coupling Chemistry. *Science* **2017**, *356*, eaaf7230.
- ⁵ Trost, B. M. Selectivity: A Key to Synthetic Efficiency *Science* **1983**, *219*, 245.
- ⁶ Green, S. A.; Crossley, S. W.; Matos, J. L.; Vásquez-Céspedes, S.; Shevick, S. L.; Shenvi, R. A. The High Chemofidelity of Metal-Catalyzed Hydrogen Atom Transfer. *Acc. Chem. Res.* **2018**, *51*, 2628–2640.
- ⁷ Liu, Y.; Han, S.-J.; Liu, W.-B.; Stoltz, B. M. Catalytic Enantioselective Construction of Quaternary Stereocenters: Assembly of Key Building Blocks for the Synthesis of Biologically Active Molecules. *Acc. Chem. Res.* **2015**, *48*, 740–751.
- ⁸ Matos, J. L. M.; Green, S. A.; Shenvi, R. A. Markovnikov Functionalization by Hydrogen Atom Transfer. *Organic Reactions* **2019**, *100*, 383.
- ⁹ Zombeck, A.; Hamilton, D. E.; Drago, R. S. Novel Catalytic Oxidations of Terminal Olefins by Cobalt(II)-Schiff Base Complexes. *J. Am. Chem. Soc.* **1982**, *104*, 6782–6784.
- ¹⁰ Corden, B. B.; Drago, R. S.; Perito, R. P. Steric and Electronic Effects of Ligand Variation on Cobalt Dioxygen Catalysts. *J. Am. Chem. Soc.* **1985**, *107*, 2903–2907.
- ¹¹ Hamilton, D. E.; Drago, R. S.; Zombeck, A. Mechanistic Studies on the Cobalt(II) Schiff Base Catalyzed Oxidation of Olefins by O₂. *J. Am. Chem. Soc.* **1987**, *109*, 374–379.
- ¹² Mukaiyama, T.; Yamada, T. Recent Advances in Aerobic Oxygenation. *Bull. Chem. Soc. Jpn.* **1995**, *68*, 17–35.

¹³ Waser, J.; Carreira, E. M. Convenient Synthesis of Alkylhydrazides by the Cobalt-Catalyzed Hydrohydrazination Reaction of Olefins and Azodicarboxylates. *J. Am. Chem. Soc.* 2004, **126**, 5676–5677.

¹⁴ Waser, J.; Carreira, E. M. Catalytic Hydro-hydrazination of a Wide Range of Alkenes with a Simple Mn Complex. *Angew. Chem., Int. Ed.* 2004, **43**, 4099–4102.

¹⁵ Waser, J.; Gaspar, B.; Nambu, H.; Carreira, E. M. Hydrazines and Azides via the Metal-Catalyzed Hydrohydrazination and Hydroazidation of Olefins. *J. Am. Chem. Soc.* 2006, **128**, 11693–11712.

¹⁶ Gaspar, B.; Carreira, E. M. Mild Cobalt-Catalyzed Hydrocyanation of Olefins with Tosyl Cyanide. *Angew. Chem., Int. Ed.* 2007, **46**, 4519–4522.

¹⁷ Gaspar, B.; Carreira, E. M. Catalytic Hydrochlorination of Unactivated Olefins with para-Toluenesulfonyl Chloride. *Angew. Chem., Int. Ed.* 2008, **47**, 5758–5760.

¹⁸ Gaspar, B.; Carreira, E. M. Cobalt Catalyzed Functionalization of Unactivated Alkenes: Regioselective Reductive C–C Bond Forming Reactions. *J. Am. Chem. Soc.* 2009, **131**, 13214–13215.

¹⁹ Collins, K. D.; Glorius, F. A robustness screen for the rapid assessment of chemical reactions *Nature Chem.* **2013**, **5**, 597–601.

²⁰ Crossley, S. W.; Obradors, C.; Martinez, R. M.; Shenvi, R. A. Mn-, Fe-, and Co-Catalyzed Radical Hydrofunctionalizations of Olefins. *Chem. Rev.* **2016**, **116**, 8912–9000.

²¹ Sweany, R. L.; Halpern, J. Hydrogenation of Alpha-Methylstyrene by Hydridopentacarbonylmanganese (I). Evidence for a Free-Radical Mechanism. *J. Am. Chem. Soc.* **1977**, **99**, 8335–8337.

²² Iwasaki, K.; Wan, K. K.; Oppedisano, A.; Crossley, S. W.; Shenvi, R. A. Simple, Chemoselective Hydrogenation with Thermodynamic Stereocontrol. *J. Am. Chem. Soc.* **2014**, **136**, 1300–1303.

²³ Wan, K. K.; Iwasaki, K.; Umotoy, J. C.; Wolan, D. W. and Shenvi, R. A. Nitrosopurines en route to potently cytotoxic asmarines. *Angew. Chem.* **2015**, **127**, 2440–2445.

²⁴ Niman, S. W.; Buono, R.; Fruman, D. A.; Vanderwal, C. D. Synthesis of a Complex Brasilicardin Analogue Utilizing a Cobalt-Catalyzed MHAT-Induced Radical Bicyclization Reaction. *Org. Lett.* **2023**, **25**, 3451–3455.

²⁵ Jiang, H.; Lai, W.; Chen, H. Generation of Carbon Radical from Iron-Hydride/Alkene: Exchange-Enhanced Reactivity Selects the Reactive Spin State. *ACS Catal.* **2019**, **9**, 6080–6086.

²⁶ van der Puyl, V.; Shenvi, R. A. Manganese-, Iron-, and Cobalt-Catalyzed Radical Alkene Hydrofunctionalization. *Base-Metal Catalysis 2* **2023**.

²⁷ Shevick, S. L.; Obradors, C.; Shenvi, R. A. Mechanistic Interrogation of Co/Ni-Dual Catalyzed Hydroarylation. *J. Am. Chem. Soc.* **2018**, **140**, 12056–12068.

²⁸ Biswas, S.; Weix, D. J. Mechanism and Selectivity in Nickel-Catalyzed Cross-Electrophile Coupling of Aryl Halides with Alkyl Halides. *J. Am. Chem. Soc.* **2013**, **135**, 16192–16197.

²⁹ Green, S. A.; Matos, J. L.; Yagi, A.; Shenvi, R. A. Branch-Selective Hydroarylation: Iodoarene–Olefin Cross-Coupling. *J. Am. Chem. Soc.* **2016**, **138**, 12779–12782.

³⁰ Green, S. A.; Vásquez-Céspedes, S.; Shenvi, R. A. Iron–Nickel Dual-Catalysis: A New Engine for Olefin Functionalization and the Formation of Quaternary Centers. *J. Am. Chem. Soc.* **2018**, **140**, 11317–11324.

³¹ Leggans, E. K.; Barker, T. J.; Duncan, K. K.; Boger, D. L. Iron(III)/NaBH₄-Mediated Additions to Unactivated Alkenes: Synthesis of Novel 20'-Vinblastine Analogues. *Org. Lett.* **2012**, **14**, 1428–1431.

³² Barker, T. J.; Boger, D. L. Fe(III)/NaBH₄-Mediated Free Radical Hydrofluorination of Unactivated Alkenes. *J. Am. Chem. Soc.* **2012**, **134**, 13588–13591.

³³ Ishikawa, H.; Colby, D. A.; Seto, S.; Va, P.; Tam, A.; Kakei, H.; Rayl, T. J.; Hwang, I.; Boger, D. L. Total Synthesis of Vinblastine, Vincristine, Related Natural Products, and Key Structural Analogues. *J. Am. Chem. Soc.* **2009**, **131**, 4904–4916.

³⁴ Lo, J. C.; Yabe, Y.; Baran, P. S. A Practical and Catalytic Reductive Olefin Coupling. *J. Am. Chem. Soc.* **2014**, **136**, 1304–1307.

³⁵ Lo, J. C.; Gui, J.; Yabe, Y.; Pan, C.-M.; Baran, P. S. Functionalized olefin cross-coupling to construct carbon–carbon bonds. *Nature* **2014**, **516**, 343–348.

³⁶ Lo, J. C.; Kim, D.; Pan, C.-M.; Edwards, J. T.; Yabe, Y.; Gui, J.; Qin, T.; Gutiérrez, S.; Giacoboni, J.; Smith, M. W.; Holland, P. L.; Baran, P. S. Fe-Catalyzed C–C Bond Construction from Olefins via Radicals. *J. Am. Chem. Soc.* **2017**, **139**, 2484–2503.

³⁷ Kim, D.; Rahaman, S. M.; Mercado, B. Q.; Poli, R.; Holland, P. L. Roles of Iron Complexes in Catalytic Radical Alkene Cross-Coupling: A Computational and Mechanistic Study. *J. Am. Chem. Soc.* **2019**, **141**, 7473–7485.

³⁸ Crossley, S. W. M.; Barabe, F.; Shenvi, R. A. Simple, chemoselective, catalytic olefin isomerization. *J. Am. Chem. Soc.* **2014**, **136**, 16788–16791.

³⁹ Shigehisa, H.; Aoki, T.; Yamaguchi, S.; Shimizu, N.; Hiroya, K.; Catalytic Hydroamination of Unactivated Olefins Using a Co Catalyst for Complex Molecule Synthesis. *J. Am. Chem. Soc.* **2013**, **135**, 10306–10309.

⁴⁰ Biswas, S.; Weix, D. J. Mechanism and Selectivity in Nickel-Catalyzed Cross-Electrophile Coupling of Aryl Halides with Alkyl Halides. *J. Am. Chem. Soc.* **2013**, *135*, 16192–16197.

⁴¹ Obradors, C.; Martinez, R. M.; Shenvi, R. A. Ph(i-PrO)SiH₂: An Exceptional Reductant for Metal-Catalyzed Hydrogen Atom Transfers. *J. Am. Chem. Soc.* **2016**, *138*, 4962–4971.

⁴² Egorova, K. S. & Ananikov, V. P. Which metals are green for catalysis? Comparison of the toxicities of Ni, Cu, Fe, Pd, Pt, Rh, and Au salts. *Ang. Chem. Int. Ed.* **2016**, *55*, 12150–12162.

⁴³ Matos, J. L.; Vásquez-Céspedes, S.; Gu, J.; Oguma, T.; Shenvi, R. A. Branch-Selective Addition of Unactivated Olefins into Imines and Aldehydes. *J. Am. Chem. Soc.* **2018**, *140*, 16976–16981.

⁴⁴ Ebisawa, K.; Izumi, K.; Ooka, Y.; Kato, H.; Kanazawa, S.; Komatsu, S.; Nishi, E.; Shigehisa, H. Catalyst- and Silane-Controlled Enantioselective Hydrofunctionalization of Alkenes by Cobalt-Catalyzed Hydrogen Atom Transfer and Radical-Polar Crossover. *J. Am. Chem. Soc.* **2020**, *142*, 13481–13490.

⁴⁵ Touney, E. E.; Foy, N. J.; Pronin, S. V. Catalytic Radical–Polar Crossover Reactions of Allylic Alcohols. *J. Am. Chem. Soc.* **2018**, *140*, 16982–16987.

⁴⁶ Zhou, X.-L.; Yang, F.; Sun, H.-L.; Yin, Y.-N.; Ye, W.-T.; Zhu, R. Cobalt-Catalyzed Intermolecular Hydrofunctionalization of Alkenes: Evidence for a Bimetallic Pathway. *J. Am. Chem. Soc.* **2019**, *141*, 7250–7255.

⁴⁷ Yin, Y.-N.; Ding, R.-Q.; Ouyang, D.-C.; Zhang, Q.; Zhu, R. Highly Chemoselective Synthesis of Hindered Amides via Cobalt-Catalyzed Intermolecular Oxidative Hydroamidation. *Nature Communications* **2021**, *12*, 2552–2562.

⁴⁸ Kochi, J. K.; Powers, J. W. Mechanism of Reduction of Alkyl Halides by Chromium(II) Complexes. Alkylchromium Species as Intermediates. *J. Am. Chem. Soc.* **1970**, *92*, 137–146.

⁴⁹ Estes, D. P.; Grills D.C.; Norton J.R.; The Reaction of Cobaloximes with Hydrogen: Products and Thermodynamics. *J Am Chem Soc.* **2014**, *136*, 17362–17365. (b) Luo, Y. R., Comprehensive Handbook of Chemical Bond Energies, CRC Press, Boca Raton, **2007**, 1.

⁵⁰ Li, G.; Han, A.; Pulling, M. E.; Estes, D. P.; Norton, J. R. Evidence for Formation of a Co–H Bond from (H₂O)₂Co(dmgBF₂)₂ under H₂: Application to Radical Cyclizations. *J. Am. Chem. Soc.* **2012**, *134*, 14662–14665.

⁵¹ Nazir, M.; Saleem, M.; Tousif, M. I.; Anwar, M. A.; Surup, F.; Ali, I.; Wang, D.; Mamadalieva, N. Z.; Alshammary, E.; Ashour, M. L.; Ashour, A. M.; Ahmed, I.; Elizbit; Green, I. R.; Hussain, H. Meroterpenoids: A Comprehensive Update Insight on Structural Diversity and Biology. *Biomolecules* **2021**, *11*, 957–1018.

⁵² Faqueti, L. G.; Farias, I. V.; Sabedot, E. C.; Monache, F. D.; Feliciano, A. S.; Schuquel, I. T. A.; Cechinel-Filho, V.; Cruz, A. B.; Meyre-Silva, C. Macrocarpal-like Compounds from *Eugenia umbelliflora* Fruits and Their Antibacterial Activity. *J. Agric. Food Chem.* **2015**, *63*, 8151–8155.

⁵³ Tran, D. N.; Cramer, N. Biomimetic Synthesis of (+)-Ledene, (+)-Viridiflorol, (-)-Palustrol, (+)-Spathulenol, and Psiguadial A, C, and D via the Platform Terpene (+)-Bicyclogermacrene. *Chem. Eur. J.* **2014**, *20*, 10654–10660.

⁵⁴ Bhunia, A.; Bergander, K.; Daniliuc, C. G.; Studer, A. Fe- Catalyzed Anaerobic Mukaiyama-Type Hydration of Alkenes using Nitroarenes. *Angew. Chem., Int. Ed.* **2021**, *60*, 8313.

⁵⁵ Nishimura, H.; Calvin, M. Essential Oil of Eucalyptus Globulus in California. *J. Agric. Food Chem.* **1979**, *27*, 432–435.

⁵⁶ Pereira, S. I.; Freire, C. S.; Neto, C. P.; Silvestre, A. J.; Silva, A. M. Chemical Composition of the Essential Oil Distilled from the Fruits Of eucalyptus Globulus Grown in Portugal. *Flavour Fragr. J.* **2005**, *20*, 407–409.

⁵⁷ San Diego Natural History Museum, San Diego County Plant Atlas, sdplantatlas.org, (accessed 2023-09-01).

⁵⁸ Liu, W.; Lavagnino, M. N.; Gould, C. A.; Alcázar, J.; MacMillan, D. W. A Biomimetic S_H2 Cross-Coupling Mechanism for Quaternary *sp*³-Carbon Formation. *Science* **2021**, *374*, 1258–1263.

⁵⁹ Tourney, E.; Cooper, R.; Bredenkamp, S.; George, D.; Pronin, S. Catalytic Radical–Polar Crossover Ritter Reaction. *ChemRxiv*, April 20, 2021. DOI: 10.26434/chemrxiv.14450580.v1.

⁶⁰ Wu, X.; Gannett, C. N.; Liu, J.; Zeng, R.; Novaes, L. F.; Wang, H.; Abruña, H. D.; Lin, S. Intercepting Hydrogen Evolution with Hydrogen-Atom Transfer: Electron-Initiated Hydrofunctionalization of Alkenes. *J. Am. Chem. Soc.* **2022**, *144*, 17783–17791.

⁶¹ Choi, J.; Pulling, M. E.; Smith, D. M.; Norton, J. R. Unusually Weak Metal–Hydrogen Bonds in HV(CO)4(P–P) and Their Effectiveness as H[•] Donors. *J. Am. Chem. Soc.*, **2008**, *130*, 4250–4252.

⁶² Fürstner, A. Iron Catalysis in Organic Synthesis: A Critical Assessment of What It Takes To Make This Base Metal a Multitasking Champion. *ACS Cent. Sci.* **2016**, *2*, 778–789.

⁶³ Woo, S.; Shenvi, R. A. Synthesis and Target Annotation of the Alkaloid GB18. *Nature* **2022**, *606*, 917–921.

⁶⁴ Thomas, B. *Galbulimima belgraveana* (F. Muell) Sprague, *galbulimima agara*. *Eleusis J. Psychoact. Plants Compd.* **1999**, *2*, 82–88.

⁶⁵ Thomas, B. Psychoactive properties of *Galbulimima* bark. *J. Psychoact. Drugs* **2005**, *37*, 109–111.

⁶⁶ Thomas, B. *Galbulimima* bark and ethnomedicine in Papua New Guinea. *P. N. G. Med. J.* **2006**, *49*, 57–59.

⁶⁷ Thomas, B. Psychoactive plant use in Papua New Guinea. *Sci. New Guin.* **2000**, *25*, 33–59.

⁶⁸ Bour, J. R.; Ferguson, D. M.; McClain, E. J.; Kampf, J. W.; Sanford, M. S. Connecting Organometallic Ni(III) and Ni(IV): Reactions of Carbon-Centered Radicals with High-Valent Organo- nickel Complexes. *J. Am. Chem. Soc.* **2019**, *141*, 8914.

⁶⁹ Wang, Y.; Wen, X.; Cui, X.; Zhang, X. P. Enantioselective radical cyclization for construction of 5-membered ring structures by metalloradical C–H alkylation. *J. Am. Chem. Soc.* **2018**, *140*, 4796.

⁷⁰ Liu, W.; Lavagnino, M. N.; Gould, C. A.; Alcázar, J.; MacMillan, D. W. C. A biomimetic SH2 cross-coupling mechanism for quaternary sp³-carbon formation. *Science* **2021**, *374*, 1258.

⁷¹ Everson, D. A.; Weix, D. J. Cross-Electrophile Coupling: Principles of Reactivity and Selectivity. *J. Org. Chem.* **2014**, *79*, 4793–4798.

⁷² Poremba, K. E.; Dibrell, S. E.; Reisman, S. E. Nickel-Catalyzed Enantioselective Reductive Cross-Coupling Reactions. *ACS Catal.* **2020**, *10*, 8237–8246.

⁷³ Hansen, E. C.; Pedro, D. J.; Wotal, A. C.; Gower, N. J.; Nelson, J. D.; Caron, S.; Weix, D. J. New Ligands for Nickel Catalysis from Diverse Pharmaceutical Heterocycle Libraries. *Nat. Chem.* **2016**, *8*, 1126–1130.

⁷⁴ Landwehr, E. M.; Baker, M. A.; Oguma, T.; Burdge, H. E.; Kawaijiri, T.; Shenvi, R. A. Concise Syntheses of GB22, GB13, and Himgaline by Cross-Coupling and Complete Reduction. *Science* **2022**, *375*, 1270–1274.

⁷⁵ Koltunov, K. Y.; Prakash, G. K. S.; Rasul, G.; Olah, A. Reactions of 5-, 6-, 7-, 8-Hydroxyquinolines and 5-Hydroxyisoquinoline with Benzene and Cyclohexane in Superacids. *J. Org. Chem.* **2002**, *67*, 4330–4336.

⁷⁶ Rinderhagen, H.; Waske, P. A.; Mattay, J. Facile Ring Opening of Siloxy Cyclopropanes by Photoinduced Electron Transfer. A New Way to β -Keto Radicals. *Tetrahedron* **2006**, *62*, 6589–6593.

⁷⁷ Aoki, S.; Fujimura, T.; Nakamura, E.; Kuwajima, I. Palladium-Catalyzed Arylation of Siloxycyclopropanes with Aryl Triflates. Carbon Chain Elongation via Catalytic Carbon–Carbon Bond Cleavage. *J. Am. Chem. Soc.* **1988**, *110*, 3296–3298.

⁷⁸ Varabyeva, N.; Barysevich, M.; Aniskevich, Y.; Hurski, A. Ti(O*i*-Pr)₄-Enabled Dual Photoredox and Nickel-Catalyzed Arylation and Alkenylation of Cyclopropanols. *Org. Lett.* **2021**, *23*, 5452–5456.

⁷⁹ Bume, D. D.; Pitts, C. D.; Lectka, T. Tandem C–C Bond Cleavage of Cyclopropanols and Oxidative Aromatization by Manganese(IV) Oxide in a Direct C–H to C–C Functionalization of Heteroaromatics. *Eur. J. Org. Chem.* **2016**, *26*–30.

⁸⁰ Luo, J.; Zhang, X.; Zhang, J. Carbazolic Porous Organic Framework as an Efficient, Metal-Free Visible-Light Photocatalyst for Organic Synthesis. *ACS Catal.* **2015**, *5*, 2250–2254.

⁸¹ Boger, D. L. The difference a single atom can make: synthesis and design at the chemistry– biology interface. *J. Org. Chem.* **2017**, *82*, 11961–11980.